DOI: 10.1002/ejic.200800855

Electroless Plating of Nickel Nanoparticles on CdS Nanowires

Le Wang,[a] Xinzheng Liu,[a] Min Yang,[a] Yingju Fan,[b] and Jinhua Zhan*[a]

Keywords: Nanocomposites / Nanostructures / Ferromagnetism / Semiconductors / Aggregation

Preparation of 1D CdS-Ni semiconductor-magnetic nanocomposites was achieved by means of electroless plating of nickel nanoparticles on CdS nanowires. Preformed CdS nanowires with a diameter of ca. 45 nm, a length up to several tens of μm were magnetically functionalised by the hydrazine-induced reduction of nickel chloride in ethylene glycol at 140 °C. It was found that nickel nanoparticles with a diameter of ca. 80 nm anchored on the nanowires without any surface pretreatment. Furthermore, a conversion process was detected and confirmed, something which is favourable for the nonepitaxial growth of Ni nanoparticles on CdS nanowires. The products prepared thereof were characterised in detail by XRD, TEM, HR-TEM and EDS techniques. Magnetic property measurements show that the nanocomposites display ferromagnetic properties at room temperature.

Introduction

Nanocomposites consisting of two important functional materials are essential for developing potential nanoelectronic and optoelectronic devices and their development represents a significant challenge in the field of nanoscience.[1–5] Materials with controlled structures and interface interactions often exhibit superior or new functional properties compared with their individual constituent counterparts. 1D Semiconductor nanostructures have attracted much research attention in recent years owning to their novel properties such as lasing action[6] and highly polarised photoluminescence which results from their particular dimensionality.[7] Over the past few years, both shape and compositional control have been applied to semiconductor nanostructures, resulting in discrete domains of different materials joined together to form anisotropic shapes.[8–13] Through functional assembly the optical, electronic,[4] magnetic and chemical properties of these semiconductor-included nanocomposites have largely been enhanced or modified. Established examples comprise various associations of semiconductors nanostructures with active inorganic components such as semiconductor analogues,[14–16] noble metals,[17–20] transition metals and magnetic nanomaterials.[21]

CdS, a direct bandgap semiconductor with a gap energy of 2.42 eV at 300 K is one of the first discovered semiconductors having a wide range of industrial applications.[22] On account of this, various CdS nanostructural materials have been generated through various routes including metal-catalysed growth, thermal evaporation, hydrothermal synthesis, etc.[23] The 1D CdS nanostructures were widely used as waveguides, optoelectronic switches, electro-optic modulators, metal-insulator-semiconductor field-effect transistors, light-emitting diodes etc. Nickel, an important ferromagnetic material,[24] has widely been used for magnetic assembly, magnetic trapping and involatile memory applications.[25] Nickel nanocrystals have been generated through various solution-phase approaches.[26] Combining magnetic properties with the inherent properties of 1D semiconductor materials might enable the exploration of novel functionality in these materials. In this article, we report an electroless plating route for the synthesis of 1D magnetically functionalised semiconductor nanocomposites in which Ni nanocrystals are anchored to CdS nanowires. No surface pretreatments were needed to introduce new surface functional groups or additional covalent and/or noncovalent interconnectivity for the deposition of Ni nanoparticles onto CdS nanowires in these experiments. The products were characterised by XRD, TEM, HR-TEM, ED and EDS techniques and the magnetic properties of the resultant 1D hybrid-nanostructures were measured. Furthermore, their formation mechanism is also discussed.

Results and Discussion

The CdS nanowires and 1D CdS-Ni hybrid nanocomposites were analysed by XRD, TEM and HRTEM to evaluate the structural characteristics. Part a of Figure 1 shows the powder XRD pattern from unmodified CdS nanowires, the peaks of which marked with "#" can be indexed to the

[a] School of Chemistry and Chemical Engineering, Shandong University,
Jinan 250100, People's Republic of China
Fax: +86-0531-8836-6280
E-mail: jhzhan@sdu.edu.cn
[b] School of Chemistry and Chemical Engineering, Jinan University,
Jinan 250020, People's Republic of China

Supporting information for this article is available on the WWW under http://www.eurjic.org or from the author.

hexagonal (wurtzite) structure (JCPDS no. 41-1049). Compared with the standard card, the diffraction peaks of (100) and (110) are relatively strong while the peak of (002) is weak which can be attributed to the fact that CdS nanowires mainly lie on the experimental cell during the XRD measurement process and have a preferential orientation along [001].[27] After nickel nanocrystals are deposited on the nanowires, additional diffraction peaks marked with an asterisk * appear in the XRD pattern (Figure 1, b) corresponding to the powder diffraction pattern for fcc nickel (JCPDS no. 04-0850). The (200) diffraction peak of fcc Ni located at $2\theta = 51.847°$ overlaps with the (112) peak of CdS.

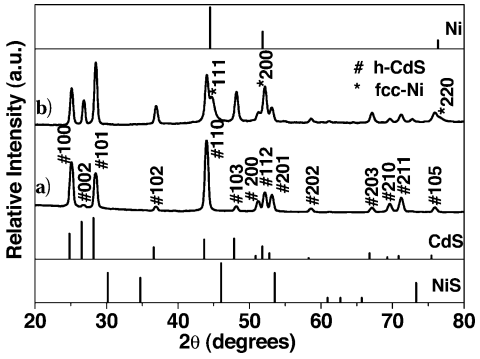

Figure 1. XRD patterns of a CdS nanowire sample before (a) and after (b) Ni growth ("#" represents h-CdS while "*" for fcc-Ni). The stick spectra represent the expected positions and intensities of the most intense XRD reflections for cubic Ni, bulk hexagonal CdS and hexagonal NiS (from top to bottom), respectively.

As seen in a low-magnification TEM image (Figure 2, a), numerous CdS nanowires with a diameter of ca. 45 nm and a length of up to several tens of micrometers are uniformly distributed on the TEM copper grid. Figure 2 (b), a highly magnified TEM image shows that the CdS nanowires commonly have a smooth surface. In Figure 2 (c), a representative TEM image of 1D CdS-Ni hybrid nanocomposites demonstrates that the CdS nanowires are decorated with nickel nanoparticles, the average diameters of which are around 80 nm. The high-resolution TEM image of the prepared 1D CdS-Ni nanocomposites, shown in Figure 2 (d), indicates that nickel nanocrystals grow along the surfaces of the CdS nanowires. The CdS nanowire is coated with a thin layer of NiS forming a shell and produced from substitution of CdS, resulting in a relatively rough surface. The thickness of the NiS shell is about 5 nm while the diameter of the CdS core is narrower than before. The solubility of bulk NiS ($K_{sp} = 1.07 \times 10^{-21}$) is higher than the solubility of bulk CdS ($K_{sp} = 8.0 \times 10^{-27}$) at room temperature.[28] It is difficult to elucidate the formation of the NiS shell through a thermodynamic cation exchange process. A kinetically driven conversion growth of NiS on the nanometre scale could occur before the deposition process of nickel nanocrystals under the present conditions. It can be suggested that Ni^{2+} ions can partially replace Cd^{2+} ions on the surface of the CdS nanowires during the experimental process in addition to the Ni nucleation and growth on the nanowire surface.

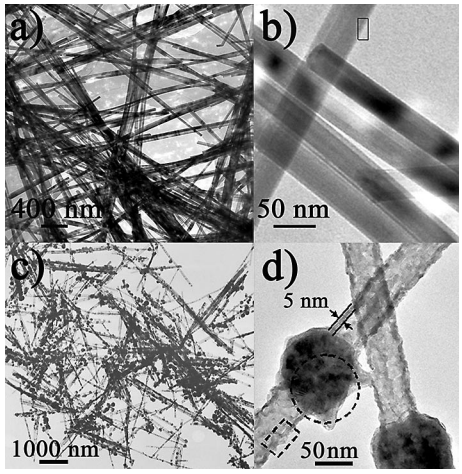

Figure 2. TEM images of CdS nanowires with average diameters of 45 nm (a,b) and nanowires loaded with 80 nm nickel nanocrystals (c,d).

The existence of an NiS layer and Ni nanoparticles on the surface of CdS nanowires was further confirmed by EDS data. EDS analyses were conducted separately on the nanowires, Ni nanoparticles and the heterojunction of the 1D nanocomposites separately labelled with circle 1, 2 and 3 in Figure 3 (a). The result in Figure 3 (b) indicates that the nanowires are mainly composed of Cd, S and Ni with a Ni/Cd/S ratio of 0.39:0.68:1 (a stoichiometry close to $Ni_xCd_{1-x}S$). The Ni nanoparticles only shows the existence of a Ni component (Figure 3c) whereas in the heterojunction part, the Ni content was richer than that in Figure 3 (b) with a Ni/Cd/S ratio of 4.5:0.88:1 (Figure 3, d). Also, a trace of oxygen was found in the EDS results, meaning a very small amount of polyglycol or some other byproduct is absorbed on the surface of the sample.[29–30] The Cu peaks were detected from the grid in TEM results.

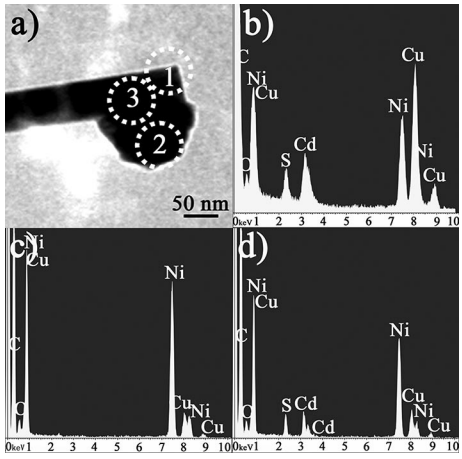

Figure 3. TEM image (a) and EDS taken from a single CdS-Ni nanocomposite in a: the nanowire part of circular region 1 (b), the nickel part of circle 2 (c) and the heterojunction part of circle 3 (d) (in figure a, both the Ni and CdS section lie horizontally on the TEM grid).

Detailed structural analysis of composite nanowires was carried out using HRTEM and electron diffraction (ED). Figure 4 (a) is a high-resolution TEM image of an individual nanowire from Figure 3 (see part a, rectangular region) which shows the multi-component composition of the nanocables. The clearly resolved interplanar distances of 3.35 Å corresponds to the (002) lattice spacing distance of hexagonal CdS, suggesting that the CdS nanowires preferentially grow along the [001] direction. Figure 4 (b) is an enlargement of the marked region in 4a, the calculated interplanar distances of 1.98 Å corresponds well to the (102) lattice spacing of h-NiS. The HRTEM image of the Ni nanoparticle in Figure 4 (c) indicates its polycrystalline nature. The corresponding select area electron diffraction (SAED) pattern of the region marked with circle in Figure 2 (d) is mainly composed of two sets of diffraction patterns. The dashed rectangle is indexed as the diffraction pattern of hexagonal CdS along the [010] zone axis and diffraction rings as those of the Ni spheres with polycrystalline nature (Figure 4d).[30] The measured lattice spacing based on the rings in the diffraction pattern can be separately indexed to the corresponding *hkl* in the PDF database. A few unassigned dots may be attributed to the neighbouring nanowire.

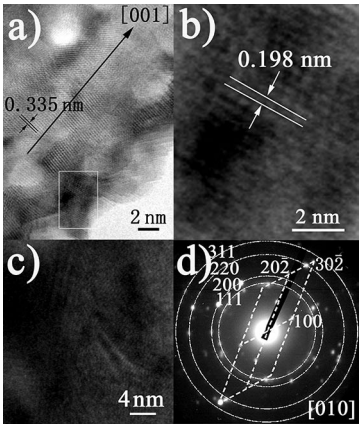

Figure 4. HRTEM images recorded in 2D: the rectangular region of the nanowire (a), an enlargement of the marked region in 4a (b) and the Ni nanoparticle (c); SAED pattern of the region marked with circle in 2D (d).

The growth of Ni nanoparticles onto CdS nanowires may be attributed to a nonepitaxial process. The nonepitaxial growth was also observed for CdS/Au and CdSe/Au hybrid nanocrystals[12,19] and, in general, is not surprising given the differences in crystal structures and lattice spacings between metal nanoparticles and the cadmium chalcogenides. On the basis of the above experimental results, the formation process of 1D CdS-Ni hybrid nanostructures can be illustrated as in Figure 5 (a). A conversion reaction has been demonstrated as a facile method for systematically varying the proportion of two chemical compositions within a single nanocrystal.[9,28,31–33] Conversion reactions occur partially and unusually fast at the surface of ionic nanocrystals after the solution had been heated in our experiments, although it is difficult for this to happen in the bulk phase.[9,28] In a parallel experiment, in the absence of hydrazine and NaOH, we obtained only CdS@NiS core/shell 1D nanostructures (Figure 6). The powder XRD pattern in Figure 6 (a) suggests the coexistence of h-CdS and h-NiS. Diffraction peaks in the top graph can be attributed purely to a combination of these two phases, the peaks marked with "#" can be indexed to h-CdS while those marked with "Δ" correspond to h-NiS. Figure 6 (d) is a high-resolution TEM image of the marked region in 6b, in which the calculated interplanar distances of 1.98 Å corresponds well with the (102) lattice spacings of h-NiS. Figure 6 (c), the SAED pattern of a single nanowire, is only consistent with the single crystalline nature of CdS indexed as the [010] zone axis. Compared with the smooth surface of a neat CdS nanowire (Figure 6, e), the relatively rough surface with structural defects in this case is produced due to the conversion reaction process. Similar conversion phenomena have already been reported and verified during the complete and fully reversible conversion of CdS(Se, Te) to Ag_2S(Se, Te)[31] and the conversion of Se@Ag_2Se to Se@MSe (M = Zn, Cd and Pb).[32–33] In most cases, tributylphosphane (TBP) and methanol acting as binding agents were employed to promote the reaction. In our experiment, EG as typical polyol played a crucial role. It can also bind to both Cd^{2+} ions in the shells and Ni^{2+} ions in solution, forming intermediate complexes to favour the forward reaction. It is worth pointing out that the substitution rate of Cd^{2+} by Ni^{2+} is very fast after heating. We found that only conversion of CdS to NiS on the surface of nanowires was observed for the sample (with, or without hydrazine and NaOH) processed for 10 min, the colour of which is still yellow. With longer reaction times, the NiS layer became a little thicker and gradually reached a constant level. After that, the thickness of the NiS shell did not increase significantly even after 24 h (Figure S1). This suggests that once a surface layer of CdS has been substituted by NiS, it caused a passivation against further Ni^{2+} attack. The anion sublattice can be partially disrupted owning to the replacement of Cd^{2+} ions by Ni^{2+} ions. Thus, structural defects such as vacancies and stacking faults appeared in the crystal structures acting as nucleation sites for the redox reaction.[19] With the reaction proceeding, nickel ripening was carried out with the consumption of the reactants in the solution and the particles became larger (Figure S2). This stage may also be related to an aggregation-driven shape-transformation process to increase the size of the nanocrystal on the nanorod.[34] Some nanoparticles could also develop into loops around the nanowires owing to the structural nature of the hexagonal-faced CdS. The six surfaces around the CdS nanowires have equal chemical activity (Figure 5, b).[35]

The field-dependent magnetisation of 1D CdS-Ni nanocomposites measured at 298 K displays hysteretic behaviour and gives *M*s, *M*r, and *H*c values of 0.02 emu g^{-1}, 0.005 emu g^{-1}, and 155.5 Oe, respectively (Figure 7, a). As indicated by the M–H curves, the ferromagnetic properties

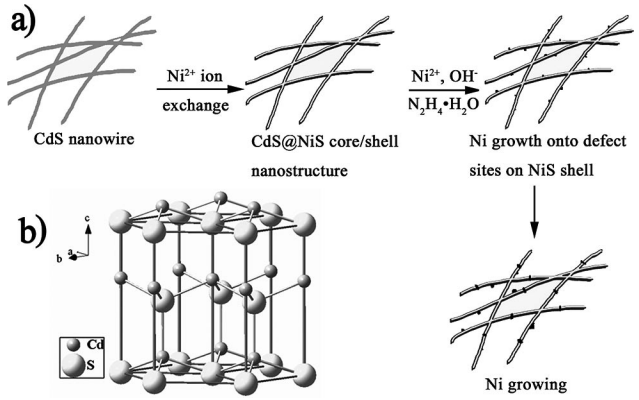

Figure 5. Schematic illustration of the formation process of 1D CdS-Ni nanocomposite (a), structural model of h-CdS (b).

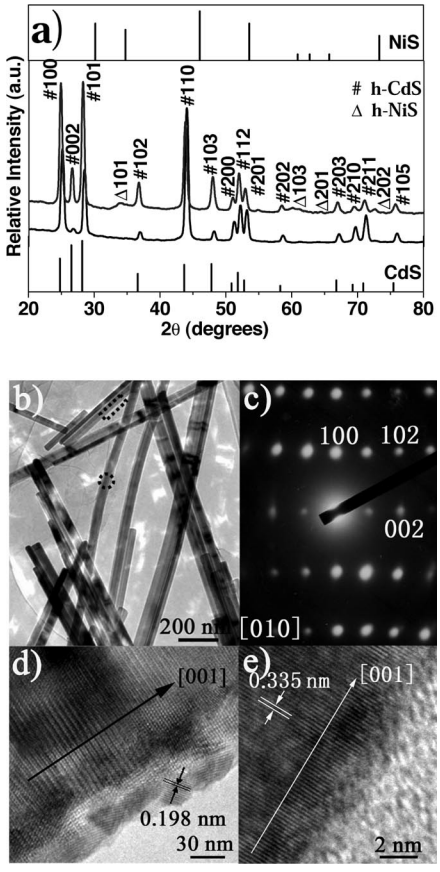

Figure 6. XRD pattern of a CdS nanowire sample before (bottom) and after (top) Ni^{2+} substitution in the absence of hydrazine and NaOH (a) ("#" represents h-CdS while "Δ" for h-NiS), the stick spectra represent the expected positions and intensities of the most intense XRD reflections for bulk hexagonal NiS and hexagonal CdS; TEM of the nanostructure after conversion (b); SAED pattern of the circular region in 6b (c). HRTEM of the rectangular region in 6b (d) and in 2b (e).

of Ni or NiS in the hybrid nanocomposites are conserved which can be explained by the cooperative effects of two types of particle interactions: magnetic-dipole and exchange interactions.[36] The magnetic properties of CdS-NiS nanowires, NiS and Ni samples synthesised at 140 °C for 12 h in the same solvent were also measured, giving *M*s, *M*r, and *H*c values of 1.43 emu g^{-1}, 0.49 emu g^{-1} and 97.9 Oe for Ni nanoparticles (Figure S3) while the magnetic properties for the formed CdS-NiS nanowires and NiS are negligible. Simultaneously, in the presence of amorphous and nonmagnetic or weakly magnetic interfaces, the saturation magnetisation was reduced substantially compared with the neat Ni samples and bulk materials.[37a,37b] The decrease in *M*s of the magnetic segments might also be attributed to the decrease in particle size and the accompanying increase in surface area.[37c] Compared with the *H*c value of bulk Ni and Ni nanoparticles,[38] the hybrid nanocomposites exhibit much enhanced coercivity owning to the effective anisotropy in the 1D exchange-coupled system formed by deposited nickel nanoparticles or the NiS shell along CdS nanowires.[36,39] As shown in Figure 7 (b), the magnetically-functionalised nanocomposites can be easily dispersed in ethanol to form a green-black solution. It has been found that the nanocomposites can be drawn to the sidewall from the solution by applying a magnet, eventually leaving a clear solution behind (part b of Figure 7, right). Figure S4a shows the magnetic manipulation of 1D CdS-Ni nanocomposites. Figure S4b is a TEM image of the dispersed 1D CdS-Ni hybrid nanocomposites after being manipulated by the magnetic fields, from which we can see that the incorporation of magnetism into the semiconductor nanostructures could make the 1D nanostructures arrange in an orderly manner with a magnetic field before the evaporation of ethanol. Magnetic functionalising of semiconductor nanostructures provides the possibility to align the nanowires exactly in the intended positions and orientations which is potentially useful in fabricating nanowire-based devices.

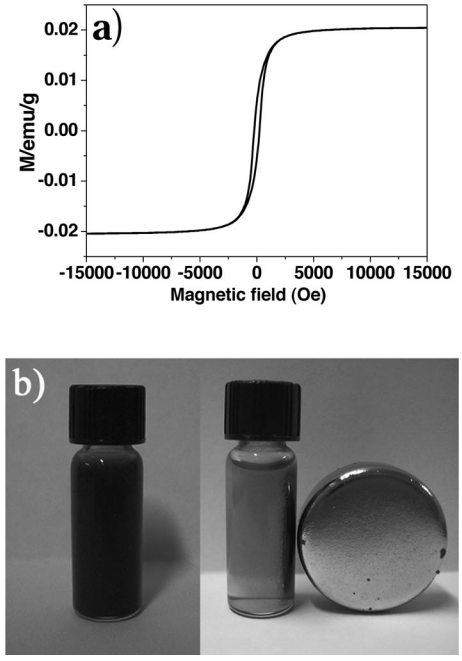

Figure 7. Hysteresis loop for 1D CdS-Ni hybrid nanocomposites (a); well-dispersed ethanol solutions of 1D CdS-Ni nanocomposites (left) and after applying a magnet to it (right) (b).

Conclusions

1D CdS-Ni semiconductor-magnetic nanocomposites have been successfully fabricated by a mild solution method. It has been demonstrated that the conversion reaction at the surface of preformed CdS nanowires provides additional nucleation sites for Ni deposition, followed by a ripening process that results in larger Ni nanocrystals around CdS. In addition, magnetic measurements show that the magnetic properties are conserved after the growth of Ni on the original CdS nanowires. The incorporation of magnetic Ni into the semiconductor makes it possible that the CdS nanowires can be aligned exactly at the intended positions or in a certain direction using a magnetic field. These types of nanocomposites are likely to find potential applications in nanoscience owing to the combination of the ferromagnetic Ni domain with the 1D semiconductor nanostructure in a hybrid nanostructure.

Experimental Section

General: The preparation of 1D CdS-Ni semiconductor-magnetic nanocomposites was achieved by means of a two-step solvothermal process. All reagents were analytical grade and were used without further purification.

Synthesis of CdS Nanowire: Uniform CdS nanowires (NWs) with diameters around 45 nm and lengths up to several μm were successfully grown through a modification of a method previously mentioned.[40] In a typical process, $Cd(S_2CNEt_2)_2$ (1.124 g, 0.1 mmol), prepared by precipitation from a stoichiometric mixture of NaS_2CNEt_2 and $CdCl_2$ in water, was added to a Teflon®-lined stainless steel autoclave with a capacity of 55 mL. The autoclave was then filled with ethylenediamine (40 mL) up to about 70% of the total volume. The autoclave was maintained at 180 °C for 24 h and then cooled to room temperature. A yellowish precipitate was collected and washed with absolute ethanol and distilled water to remove residual organic solvents. The final products were dried in a vacuum at 70 °C for 6 h in preparation for further characterisation.

Synthesis of 1D CdS-Ni Semiconductor-Magnetic Nanocomposites: 1D CdS-Ni nanocomposites were prepared by controlled Ni growth onto preformed CdS nanowires. As a general procedure, CdS NWs (0.03 g, 0.2 mmol) were well-dispersed in an EG/H_2O (45 mL, 5:1 v/v) mixture solvent under sonication. Then $NiCl_2{\cdot}6H_2O$ (0.1 g, 0.4 mmol), $N_2H_4{\cdot}H_2O$ (0.48 g, 8 mmol) and an appropriate amount of 1.0 M NaOH solution were added in sequence. The resultant mixture was loaded into a 55 mL Teflon®-lined autoclave. The autoclave was sealed and maintained at 140 °C for 12 h. After the reaction was complete, the autoclave was cooled to room temperature naturally. The resultant solid products were collected, washed with absolute ethanol and distilled water several times and then dried in vacuo at 70 °C for 6 h.

Characterisation: The crystal structure of the product was determined using an X-ray diffractometer (Bruker D8) fitted with a graphite monochromator and Cu-K_α radiation (λ = 1.5418 Å) in the range of 20–80° at room temperature while the tube voltage and electric current were held at 40 kV and 20 mA, respectively. The morphology and microstructure of the products were determined by TEM (JEM-100CXII) with an acceleration voltage of 80 kV and high-resolution TEM (HR-TEM, JEOL-2100) with an acceleration voltage of 200 kV, the equipment being fitted with an energy-dispersive X-ray spectrometer (EDS). Magnetisation measurements of the nanocomposites were performed with a Micromag 2900 instrument at room temperature under an ambient atmosphere. The nanocomposite powders were pressed into the thin slices.

Supporting Information (see also the footnote on the first page of this article): HRTM images of CdS/NiS core-shell nanowires, TEM images of 1D CdS/Ni nanocomposites, magnetic properties of Ni nanocrystals and 1D CdS/Ni nanocomposites.

Acknowledgments

Helpful discussion with Prof. Yitai Qian and financial support from National Natural Science Found of China (NSFC 20501014), Program for New Century Excellent Talents in University (NCET) and National Basic Research Program of China (973 Program 2005CB623601, 2007CB936602) is gratefully acknowledged.

[1] P. D. Cozzoli, T. Pellegrino, L. Manna, *Chem. Soc. Rev.* **2006**, *35*, 1195–1208.
[2] M. S. Gudiksen, L. J. Lauhon, J. Wang, D. C. Smith, C. M. Lieber, *Nature* **2002**, *415*, 617–620.
[3] R. He, M. Law, R. Fan, F. Kim, P. Yang, *Nano Lett.* **2002**, *2*, 1109–1112.
[4] Y. Wu, J. Xiang, C. Yang, W. Lu, C. M. Lieber, *Nature* **2004**, *430*, 61–65.
[5] Y. Huang, X. Duan, Q. Wei, Y. Cui, L. J. Lauhon, K. H. Kim, C. M. Lieber, *Science* **2001**, *294*, 1313–1317.
[6] a) M. H. Huang, S. Mao, H. Feick, H. Yan, Y. Wu, H. Kind, E. Weber, R. Russo, R. P. Yang, *Science* **2001**, *292*, 1897–1899; b) J. Ding, J. A. Zapien, W. Chen, Y. Lifshitz, S. T. Lee, *Appl. Phys. Lett.* **2004**, *85*, 2361–2363.
[7] J. Wang, M. S. Gudiksen, X. Duan, Y. Cui, C. M. Lieber, *Science* **2001**, *293*, 1455–1457.
[8] D. J. Milliron, S. M. Hughes, Y. Cui, L. Manna, J. Li, L. Wang, A. P. Alivisatos, *Nature* **2004**, *430*, 190–195.
[9] R. D. Robinson, B. Sadtler, D. O. Demchenko, C. K. Erdonmez, L. Wang, A. P. Alivisatos, *Science* **2007**, *317*, 355–358.
[10] F. Shieh, A. E. Saunders, B. A. Korgel, *J. Phys. Chem. B* **2005**, *109*, 8538–8542.
[11] D. V. Talapin, R. Koeppe, S. Goetzinger, A. Kornowski, J. M. Lupton, A. L. Rogach, O. Benson, J. Feldmann, H. Weller, *Nano Lett.* **2003**, *3*, 1677–1681.
[12] T. Mokari, E. Rothenberg, I. Popov, R. Costi, U. Banin, *Science* **2004**, *304*, 1787–1790.
[13] H. Kim, M. Achermann, L. P. Balet, J. A. Hollingsworth, V. I. Klimov, *J. Am. Chem. Soc.* **2005**, *127*, 544–546.
[14] Y. Hsu, S. Lu, Y. Lin, *Adv. Funct. Mater.* **2005**, *15*, 1350–1357.
[15] D. V. Talapin, I. Mekis, S. Gotzinger, A. Kornowski, O. Benson, H. Weller, *J. Phys. Chem. B* **2004**, *108*, 18826–18831.
[16] X. Peng, M. C. Schlamp, A. V. Kadavanich, A. P. Alivisatos, *J. Am. Chem. Soc.* **1997**, *119*, 7019–7029.
[17] A. Salant, E. A. Sadovsky, U. Banin, *J. Am. Chem. Soc.* **2006**, *128*, 10006–10007.
[18] T. Mokari, A. Aharoni, I. Popov, U. Banin, *Angew. Chem. Int. Ed.* **2006**, *45*, 8001–8005.
[19] a) A. E. Saunders, I. Popov, U. Banin, *J. Phys. Chem. B* **2006**, *110*, 25421–25429; b) T. Mokari, C. G. Sztrum, A. Salant, E. Rabani, U. Banin, *Nat. Mater.* **2005**, *4*, 855–863.
[20] P. D. Cozzoli, M. L. Curri, C. Giannini, A. Agostiano, *Small* **2006**, *2*, 413–421.
[21] a) M. Casavola, R. Buonsanti, G. Caputo, P. D. Cozzoli, *Eur. J. Inorg. Chem.* **2008**, 837–854; b) H. Gu, R. Zheng, X. Zhang, B. Xu, *J. Am. Chem. Soc.* **2004**, *126*, 5664–5665; c) S. W. Lee, M. C. Jeong, J. M. Myoung, G. S. Chae, I. J. Chung, *Appl. Phys. Lett.* **2007**, *90*, 133115–3; d) M. Casavola, V. Grillo, E. Carlino, C. Giannini, F. Gozzo, E. F. Pinel, M. A. Garcia, L.

Manna, R. Cingolani, P. D. Cozzoli, *Nano Lett.* **2007**, *7*, 1386–1395; e) R. Buonsanti, V. Grillo, E. Carlino, C. Giannini, M. L. Curri, C. Innocenti, C. Sangregorio, K. Achterhold, F. G. Parak, A. Agostiano, P. D. Cozzoli, *J. Am. Chem. Soc.* **2006**, *128*, 16953–16970.

[22] a) Q. H. Xiong, G. Chen, J. D. Acord, X. Liu, J. J. Zengel, H. R. Gutierrez, J. M. Redwing, L. C. Lew Yan Voon, B. Lassen, P. C. Eklund, *Nano Lett.* **2004**, *4*, 1663–1668; b) M. Chen, Y. Xie, J. Lu, Y. Xiong, S. Zhang, Y. Qian, X. Liu, *J. Mater. Chem.* **2002**, *12*, 748–753.

[23] a) X. F. Duan, C. M. Lieber, *Adv. Mater.* **2000**, *12*, 298–302; b) C. J. Barrelet, Y. Wu, D. C. Bell, C. M. Lieber, *J. Am. Chem. Soc.* **2003**, *125*, 11498–11499; c) C. Ye, G. Meng, Y. Wang, Z. Jiang, L. Zhang, *J. Phys. Chem. B* **2002**, *106*, 10338–10341; d) Y. Wang, G. Meng, L. Zhang, C. Liang, J. Zhang, *Chem. Mater.* **2002**, *14*, 1773–1777.

[24] a) K. Nielsch, R. B. Wehrspohn, J. Barther, J. Kirschner, S. F. Fischer, H. Kronmuller, T. Schweinbock, D. Weiss, U. Gosele, *J. Magn. Magn. Mater.* **2002**, *249*, 251–256; b) N. Cordente, M. Respaud, F. Senocq, M. J. Casanove, C. Amiens, B. Chaudret, *Nano Lett.* **2001**, *1*, 565–568; c) J. C. Bao, C. Y. Tie, Z. Xu, Q. F. Zhou, D. Shen, Q. Ma, *Adv. Mater.* **2001**, *13*, 1631–1633.

[25] A. K. Bentley, J. S. Trethewey, A. B. Ellis, W. C. Crone, *Nano Lett.* **2004**, *4*, 487–490; F. M. Yang, T. C. Chang, *Appl. Phys. Lett.* **2007**, *90*, 222104.

[26] a) M. Han, Q. Liu, J. He, Y. Song, Z. Xu, J. M. Zhu, *Adv. Mater.* **2007**, *19*, 1096–1100; b) X. Ni, Q. Zhao, H. Zheng, B. Li, J. Song, D. Zhang, X. Zhang, *Eur. J. Inorg. Chem.* **2005**, 4788–4793; c) N. Cordente, M. Respaud, F. Senocq, M. J. Casanove, C. Amiens, B. Chaudret, *Nano Lett.* **2001**, *1*, 565–568.

[27] J. Zhan, X. Yang, D. Wang, S. Li, Y. Xie, Y. Xia, Y. Qian, *Adv. Mater.* **2000**, *12*, 1348–1351.

[28] W. Zhu, W. Wang, J. Shi, *J. Phys. Chem. B* **2006**, *110*, 9785–9790.

[29] J. Bao, Y. Liang, Z. Xu, L. Si, *Adv. Mater.* **2003**, *15*, 1832–1835.

[30] Q. Liu, H. Liu, M. Han, J. Zhu, Y. Liang, Z. Xu, Y. Song, *Adv. Mater.* **2005**, *17*, 1995–1999.

[31] D. H. Son, S. M. Hughes, Y. Yin, A. P. Alivisatos, *Science* **2004**, *306*, 1009–1012.

[32] U. Jeong, J. U. Kim, Y. Xia, Z. Li, *Nano Lett.* **2005**, *5*, 937–942.

[33] P. H. C. Camargo, Y. H. Lee, U. Jeong, Z. Zou, Y. Xia, *Langmuir* **2007**, *23*, 2985–2992.

[34] J. Zhan, H. Lin, C. Mou, *Adv. Mater.* **2003**, *15*, 621–623.

[35] a) L. Yin, Y. Bando, J. Zhan, M. Li, D. Golberg, *Adv. Mater.* **2005**, *17*, 1972–2977; b) A. Figuerola, A. Fiore, R. D. Corato, A. Falqui, C. Giannini, E. Micotti, A. Lascialfari, M. Corti, R. Cingolani, T. Pellegrino, P. D. Cozzoli, L. Manna, *J. Am. Chem. Soc.* **2008**, *130*, 1477–1487.

[36] R. S. Iskhakov, S. V. Komagortsev, A. D. Balaev, A. V. Okotrub, A. G. Kudashov, V. L. Kuznetsov, Y. V. Butenko, *JETP Lett.* **2003**, *78*, 236–240.

[37] a) S. H. Wu, D. H. Chen, *J. Colloid Interface Sci.* **2003**, *259*, 282–286; b) J. H. Hwang, V. P. Dravid, M. H. Teng, J. J. Host, B. R. Elliott, D. L. Johnson, T. O. Mason, *J. Mater. Res.* **1997**, *12*, 1076–1082; c) V. P. M. Shafi, A. Gedanken, R. Prozorov, J. Balogh, *Chem. Mater.* **1998**, *10*, 3445–3450.

[38] a) Z. Liu, S. Li, Y. Yang, S. Peng, Z. Hu, Y. Qian, *Adv. Mater.* **2003**, *15*, 1946–1948; b) H. T. Zhang, G. Wu, X. H. Chen, *Mater. Lett.* **2005**, *59*, 3728–3731.

[39] E. N. Konyushenko, N. E. Kazantseva, J. Stejskal, M. Trchová, J. Kovářová, I. Sapurina, M. M. Tomishko, O. V. Demicheva, J. Prokeš, *J. Magn. Magn. Mater.* **2008**, *320*, 231–240.

[40] P. Yan, Y. Xie, Y. Qian, X. Liu, *Chem. Commun.* **1999**, *86*, 1293–1294.

Received: August 26, 2008
Published Online: January 28, 2009

